Reduced expression of the Nodal co-receptor Oep causes loss of mesendodermal competence in zebrafish

Pavel Vopalensky, Sabrina Pralow and Nadine L. Vastenhouw*

ABSTRACT

The activation of specific gene expression programs depends on the presence of the appropriate signals and the competence of cells to respond to those signals. Although it is well established that cellular competence is regulated in space and time, the molecular mechanisms underlying the loss of competence remain largely unknown. Here, we determine the time window during which zebrafish prospective ectoderm loses its ability to respond to Nodal signals, and show that this coincides with a decrease in the levels of the Nodal co-receptor One-eyed pinhead (Oep). Bypassing Oep using a photoactivatable receptor, or an Oep-independent ligand, allows activation of Nodal target genes for an extended period of time. These results suggest that the reduced expression of Oep causes the loss of responsiveness to Nodal signals in the prospective ectoderm. Indeed, extending the presence of Oep prolongs the window of competence to respond to Nodal signals. Our findings suggest a simple mechanism in which the decreasing level of one component of the Nodal signaling pathway regulates the loss of mesendodermal competence in the prospective ectoderm.

KEY WORDS: Competence, Mesendoderm, Nodal, Activin, Oep, Tdgf1, *Danio rerio*

INTRODUCTION

During embryogenesis, the activation of specific gene expression programs results in the generation of functionally differentiated cells. In vertebrates, this process is largely driven by cell signaling (Gilbert, 2010). During the formation of the three germ layers (ectoderm, mesoderm and endoderm), Nodal signaling plays an important role in inducing pluripotent blastomeres to become mesendoderm (Dubrulle et al., 2015; Feldman et al., 2000, 1998; Kunwar et al., 2003; Thisse et al., 2000). Although all cells of the embryo are initially competent to respond to Nodal, blastomeres of the prospective ectoderm lose mesendodermal competence over time (Grainger and Gurdon, 1989; Ho and Kimmel, 1993). The mechanisms underlying this loss of mesendodermal competence are not fully understood.

Given the structure of the Nodal signaling pathway, the loss of competence in the prospective ectoderm could be caused by extracellular, cytoplasmic or nuclear changes. Nodal morphogens (reviewed by Schier, 2009) are extracellular ligands of the TGFβ signaling pathway that act through type I and type II Activin receptors. Upon ligand binding, the receptors phosphorylate

Max Planck Institute of Molecular Cell Biology and Genetics, Pfotenhauerstraße 108, 01307 Dresden, Germany.

*Author for correspondence (vastenhouw@mpi-cbg.de)

P.V., 0000-0002-6171-1557; N.L.V., 0000-0001-8782-9775

cytoplasmic Smad2, which in turn recruits Smad4 and enters the nucleus. Here, the Smad2/4 complex associates with additional transcription factors such as FoxHI and Mixer (Kunwar et al., 2003; Slagle et al., 2011), as well as chromatin modifiers (Dahle et al., 2010; Morikawa et al., 2013; Xi et al., 2011), to regulate the transcription of Nodal target genes. Experiments performed in *Xenopus* animal caps have suggested that changes in the cytoplasm and nucleus play a role in the loss of mesendodermal competence. Phosphorylation of the linker region of Smad2 results in its nuclear exclusion and, consequently, in the loss of competence (Grimm and Gurdon, 2002). Furthermore, the biological activity of Smad4 in the ectoderm is attenuated by ubiquitylation by Ectodermin (Dupont et al., 2005). In the nucleus, accumulation of the somatic linker histone H1 selectively silences genes required for mesoderm differentiation (Steinbach et al., 1997), an effect that depends on the ratio between histone H3.3 and H1 (Lim et al., 2013). Similarly, trimethylation of histone H3 lysine 27 has been suggested to inhibit mesendoderm differentiation in zebrafish embryos (Shiomi et al., 2017). A role for extracellular factors, however, was not addressed in these studies, and it remains unclear whether these also play a role in the loss of competence.

The extracellular factors required to respond to Nodal signaling include the Activin receptors, as well as Nodal co-receptors from the EGF-CFC family (Cheng et al., 2003; Chu and Shen, 2010; Dorey and Hill, 2006; Fleming et al., 2013; Gritsman et al., 1999; Schier et al., 1997). For example, the zebrafish Nodal co-receptor One-eyed pinhead (Oep; also known as Tdgf1) is essential to mediate the interaction between Nodal ligand and receptor (Gritsman et al., 1999; Zhang et al., 1998), and *oep* mutants show severe defects in mesendoderm specification (Schier et al., 1997). The expression of *oep* in the prospective ectoderm decreases during gastrulation (van Boxtel et al., 2015; Zhang et al., 1998), suggesting that a reduction in *oep* expression might play a role in the loss of mesendodermal competence. In previous studies, this aspect would not have been detected because either Activin or constitutively active Smad2 was used to activate the Nodal signaling pathway. In contrast to Nodal protein-mediated induction, these strategies do not require EGF-CFC co-receptors to activate Nodal signaling (Gritsman et al., 1999). Thus, it remains unclear whether the reduced expression of *oep* is involved in the loss of mesendodermal competence.

Here we analyzed how mesendodermal competence in zebrafish prospective ectoderm is lost during gastrulation, and show that it is due to a decreasing expression level of the Nodal co-receptor Oep.

RESULTS AND DISCUSSION

Responsiveness of the prospective ectoderm to Nodal is lost between shield stage and 75% epiboly

To dissect the molecular changes underlying the loss of responsiveness to Nodal signals, we investigated the time window in which competence is lost. It has previously been shown that injection of Nodal protein into the intercellular space can induce

Smad2 phosphorylation and mesendodermal gene expression in the prospective ectoderm (Dubrulle et al., 2015). We delivered recombinant human NODAL protein (rhNodal) at 50% epiboly [5.3 hours post fertilization (hpf)] and analyzed the expression of Nodal target genes by *in situ* hybridization 1.5 h later (Fig. 1A). As expected, rhNodal injection led to ectopic expression of mesendodermal markers *no tail* (*ntl*; also known as *T* or *tbxta/b*) (Schulte-Merker et al., 1994), *sebox* (Poulain and Lepage, 2002) and *bhikhari* (*bhik*) (Vogel and Gerster, 1999) (Fig. 1B, Fig. S1). In addition to activating Nodal target genes, rhNodal inhibited the expression of the ectodermal markers *sox2* and *sox3* (Fig. 1C). This is consistent with the known inhibitory effect of Nodal signaling on ectodermal fate (Bennett et al., 2007).

Next, to identify the time point when competence is lost, we injected rhNodal at later developmental stages and analyzed ectopic *ntl* expression. rhNodal was able to induce *ntl* expression in animal cap cells until late shield stage, but this ability was lost at 75% epiboly (Fig. 1D). This might explain a previous observation that prospective ectodermal cells are committed to an ectodermal fate at 8 hpf (75% epiboly) (Ho and Kimmel, 1993). In summary, zebrafish prospective ectoderm cells lose their responsiveness to Nodal between shield stage (6 hpf) and 75% epiboly (8 hpf).

Loss of responsiveness to Nodal in the prospective ectoderm is caused by extracellular changes

Next, we asked whether the loss of Nodal responsiveness at 75% epiboly is caused by extracellular or intracellular changes. We used photoswitchable Activin receptors I and II, which activate the Nodal signaling pathway upon blue light illumination (OptoAcvRs) (Sako et al., 2016) (Fig. 2A). Owing to the lack of extracellular domains, the activation of OptoAcvRs is uncoupled from all extracellular influences. We injected mRNAs encoding the OptoAcvR receptors at the 1-cell stage, bypassing the need for endogenous Activin receptors. Thus, the ability of OptoAcvR-injected embryos to induce transcription of mesendodermal genes depends solely on the cytoplasmic portion of the Nodal signaling pathway and the nuclear context. Upon OptoAcvR injection, we illuminated embryos for 1.5 h starting at 50% epiboly, shield or 75% epiboly stage (see Fig. S2 for a detailed description of this approach). Light stimulation induced ectopic *ntl* expression at all stages examined, including 75% epiboly, whereas control embryos that were kept in the dark did not show any ectopic *ntl* expression (Fig. 2B). The ability of OptoAcvR, but not rhNodal, to induce *ntl* at 75% epiboly suggests that the loss of Nodal responsiveness is caused by changes at the extracellular level.

Reduced expression of the Nodal co-receptor Oep causes loss of responsiveness to Nodal in the prospective ectoderm

The Nodal co-receptor Oep is an important competence factor for Nodal signaling. The reduced levels of *oep* mRNA observed during gastrulation in the prospective ectoderm (van Boxtel et al., 2015; Zhang et al., 1998) suggest that a decrease in the *oep* expression level might be involved in the loss of competence. To test this hypothesis, we carefully analyzed the spatiotemporal expression pattern of *oep* during gastrulation (Fig. 3A). This revealed that the decline in *oep* expression levels within the prospective ectoderm temporally coincides with the loss of responsiveness to rhNodal injection.

To test whether the reduced expression of *oep* is responsible for the loss of responsiveness to Nodal at this stage, we attempted to induce expression of Nodal target genes by intercellular injection of Activin A, a Nodal-related ligand that does not require Oep to activate the Nodal pathway. We injected Activin A at 50%, shield or
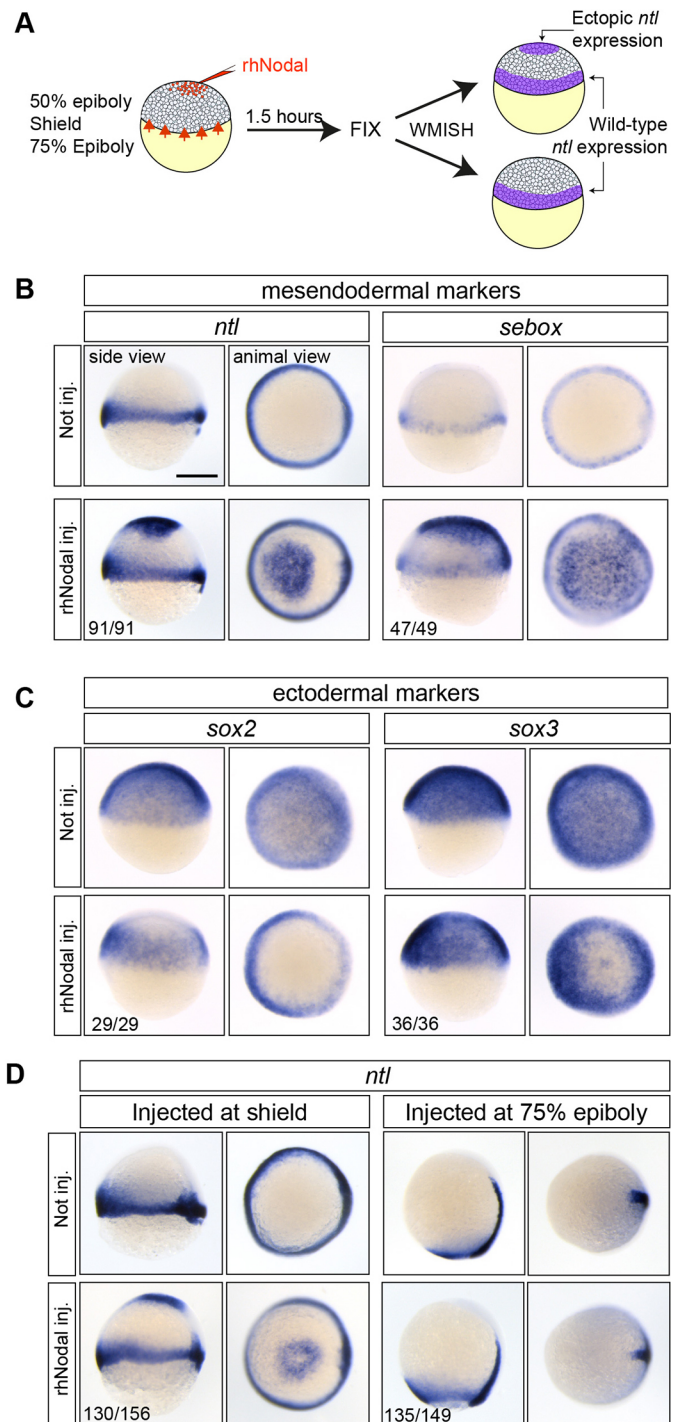
Fig. 1. Responsiveness to Nodal is lost between shield stage and 75% epiboly. (A) Experimental setup. WMISH, whole-mount *in situ* hybridization. (B,C) rhNodal induces ectopic expression of mesendodermal markers (*ntl* and *sebox*) (B) and inhibits the expression of ectodermal markers (*sox2* and *sox3*) (C) during zebrafish embryogenesis. (D) rhNodal ectopically induces *ntl* within the animal cap region at shield stage but not at 75% epiboly. The number of embryos with the indicated expression pattern among the total examined in two (*sebox*, *sox2*, *sox3*) or four (*ntl*) biological replicates is shown. All side views are shown with dorsal towards the right. Scale bar: 250 µm.

75% epiboly and analyzed embryos for expression of *ntl* (Fig. 3B), *bhik* and *gsc* (Fig. S3) after 1.5 h. Injection of Activin A led to ectopic induction of all genes within the prospective ectoderm at early stages as well as at 75% epiboly. Taken together, these data
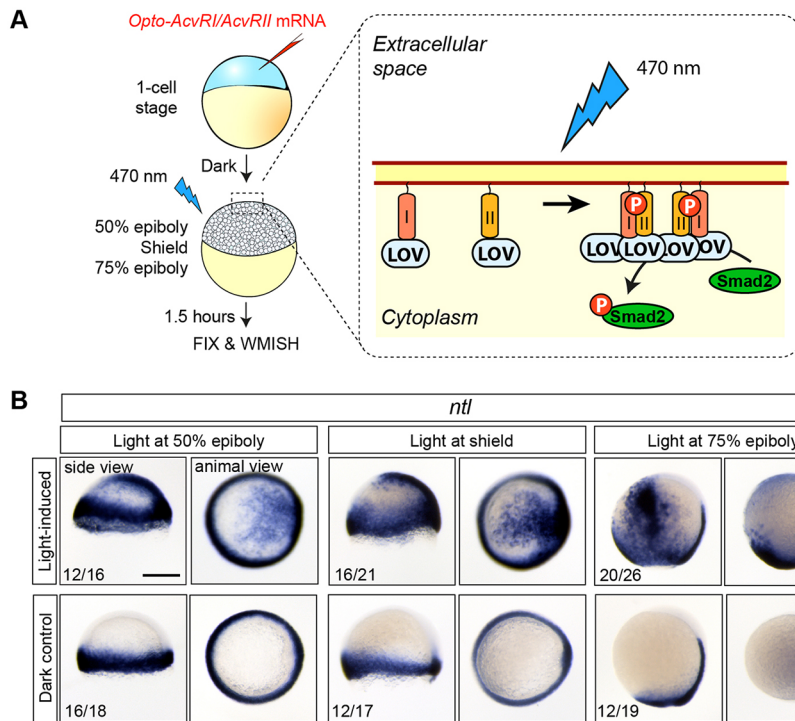
Fig. 2. Loss of Nodal competence at 75% epiboly is caused by changes in the extracellular part of the pathway. (A) Experimental setup. I and II, Activin A receptor type I and II intracellular domains; LOV, light-oxygen-voltage domain. (B) Photoactivation of OptoAcvRs results in ectopic *ntl* expression at all stages examined. Ectopic *ntl* induction was not observed in control embryos that were kept in the dark. The number of embryos with the indicated expression pattern among the total number examined in two biological replicates is shown. All side views are shown with dorsal towards the right. Scale bar: 250 µm.

suggest that loss of Nodal responsiveness in the prospective ectoderm at 75% epiboly is caused by the reduced expression of *oep*.

If the disappearance of Oep from the prospective ectoderm were causing the loss of responsiveness to Nodal, extending the expression of *oep* would be expected to prolong the window of competence. We injected mRNA encoding Oep into 1-cell stage embryos and observed elevated levels of *oep* mRNA throughout

gastrulation stages (Fig. S3A, compare with Fig. 3A). We then injected rhNodal into the intracellular space of the animal pole of *oep*-injected embryos at 50% epiboly, shield or 75% epiboly. As predicted, the *oep* mRNA-injected embryos ectopically expressed *ntl*, *gsc* and *bhik* at 75% epiboly (Fig. 3C,D, Fig. S3). Control embryos that were injected with *egfp* instead of *oep* mRNA did not show ectopic *ntl*, *gsc* and *bhik* induction at 75% epiboly (Fig. 3C,D, Fig. S3). The observation that extending *oep* expression is sufficient
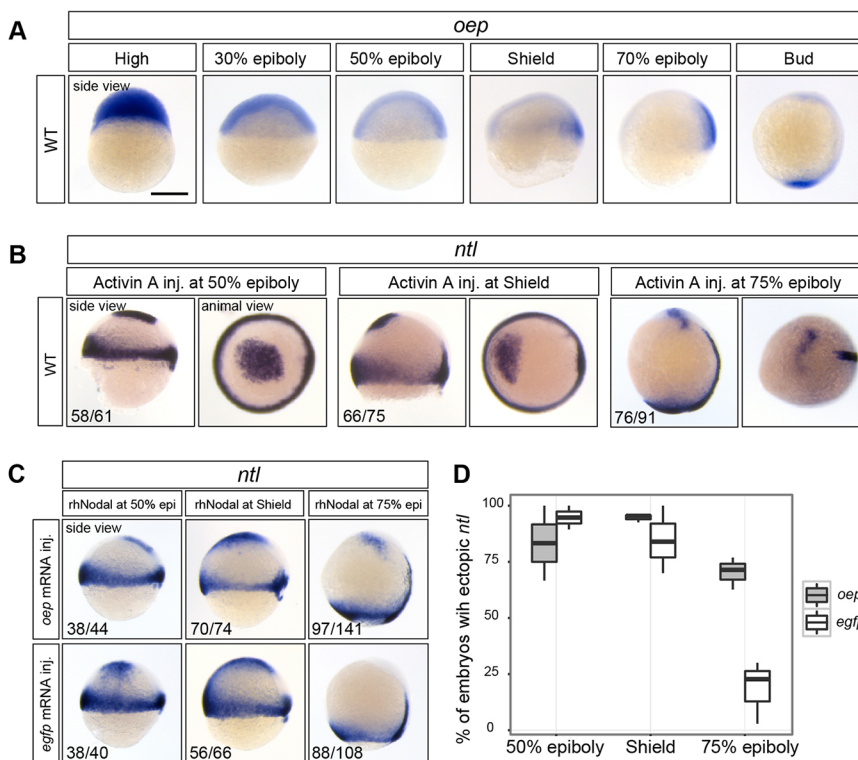
Fig. 3. Increasing the level of *oep* mRNA prolongs the window of responsiveness to Nodal. (A) Time series of *oep* expression. (B) Intercellular injection of Activin A induces ectopic *ntl* expression in the animal cap at 50%, shield and 75% epiboly. (C) In *oep*-injected embryos, but not *egfp*-injected control embryos, rhNodal is able to induce ectopic *ntl* at 75% epiboly. (D) Box plot showing the fraction of embryos with ectopic *ntl* expression (based on data shown in C). The number of embryos with the indicated expression among the total number examined in experiments performed in duplicate (B) or triplicate (C) is indicated. All side views are shown with dorsal towards the right. Scale bar: 250 µm.

to prolong the window of competence provides a functional demonstration of the central role of Oep levels in determining when mesendodermal competence is lost.

Decrease in the expression level of Oep in the prospective ectoderm is a result of embryo-wide degradation of maternally provided *oep* mRNA

Next, we analyzed how *oep* is lost in the prospective ectoderm. Our data show that *oep* expression levels decrease in the prospective ectoderm but remain high in the mesendoderm (Fig. 3A). This suggests two potential mechanisms for the decrease in *oep* expression in the prospective ectoderm. Either maternal *oep* mRNA is specifically degraded in the ectoderm, or maternal *oep* transcripts are degraded throughout the entire embryo and the gene is zygotically transcribed in the mesendoderm. In the latter case, inhibiting zygotic transcription would result in the loss of *oep* expression in the entire embryo. To test this, we inhibited transcription between dome stage and 60% epiboly using flavopiridol, a drug that inhibits RNA polymerase II elongation (Bensaude, 2011; Yang et al., 2016) (Fig. 4A). We selected this time window because zygotic transcription of *oep* has started at dome, and at 60% epiboly *oep* is differentially expressed. No *oep* expression was detected in flavopiridol-treated embryos, whereas control embryos showed *oep* expression in mesendoderm, as observed in wild-type embryos (Fig. 4B). To confirm this result, we analyzed the levels of nascent *oep* transcripts by RT-qPCR at 60% epiboly and observed a significant decrease in flavopiridol-treated compared with untreated embryos (Fig. 4C). These results are in agreement with a previous study showing that zygotic *oep* deletion mutants completely lack mesendodermal *oep* expression (Zhang et al., 1998). Thus, the decrease of *oep* expression in the prospective ectoderm is a consequence of embryo-wide degradation of maternal *oep* transcripts.

The embryo-wide degradation of maternally loaded *oep* mRNA raises the question of how this is regulated. The stability of maternally loaded mRNAs in zebrafish is influenced by the presence of miR-430 target sites, RNA methylation, and codon composition (Kontur and Giraldez, 2017). A search for miR-430 target sites in the 3′UTR of *oep* resulted in only one hit (Fig. S4A), which is much less than generally found in transcripts that depend on miR-430 for their degradation (Giraldez et al., 2006). In agreement with this, our analysis of a previously published dataset (Giraldez et al., 2006) suggests that *oep* transcripts are not destabilized by miR-430 (Fig. S4B). Similarly, m6A-dependent maternal mRNA clearance does not seem to play a role in the degradation of maternally loaded *oep* mRNA, as depletion of the m6A-binding protein Ythdf2 does not lead to any increase in *oep* mRNA (Fig. S4C) (Zhao et al., 2017). The codon composition of the *oep* coding sequence, however, is among the most destabilizing found in zebrafish genes (Fig. 4D). This suggests that the degradation of *oep* during early zebrafish embryogenesis is due to the use of codons that destabilize mRNA. Together, these data show that the decrease of *oep* expression in the prospective ectoderm is a consequence of embryo-wide degradation of *oep* transcripts, at least partially mediated by an abundance of destabilizing codons.

Our study shows that reduced expression of the Nodal co-receptor *oep* in the prospective ectoderm results in the loss of mesendodermal competence. We note that our analysis of *oep* mRNA expression might not reflect the functionally relevant level of Oep protein. However, the observation that the competence window is extended upon *oep* mRNA overexpression suggests that at 75% epiboly, Oep protein is normally reduced to levels that do not support functional
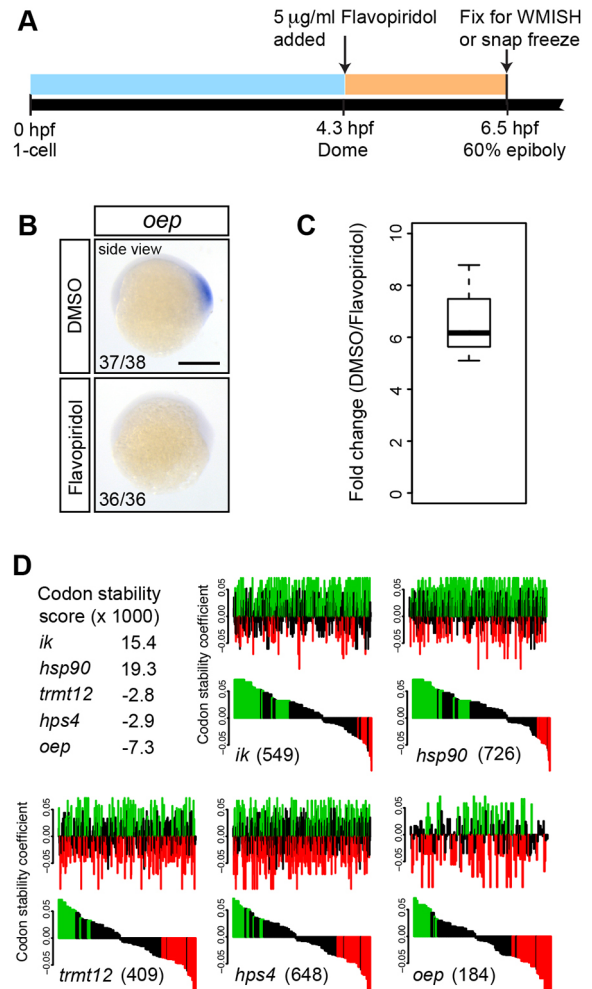
Fig. 4. Maternally loaded *oep* mRNA is globally degraded, at least partially due to the abundance of destabilizing codons. (A) Experimental setup. (B) Embryos treated with flavopiridol lack *oep* expression at 60% epiboly. The number of embryos with the indicated expression pattern among the total number examined in three biological replicates is shown. All side views are shown with dorsal towards the right. Scale bar: 250 µm. (C) RT-qPCR analysis of nascent *oep* transcript in control versus flavopiridol-treated embryos. Data are normalized to *eif4g2a*. The experiment was performed in biological triplicate. (D) *oep* coding sequence is highly enriched for destabilizing codons. The codon stability score of *oep* is lower than that of highly stable (*ik* and *hsp90*) and even highly unstable (*trmt12* and *hps4*) mRNAs as identified by Bazzini et al. (2016). The distribution of stabilizing (green) and destabilizing (red) codons along the coding sequence is shown (top), along with the same data sorted by codon stability score (bottom). The number of codons in the coding sequence is indicated in parentheses for each gene. See the supplementary Materials and Methods for further details.

signaling. The initial competence of all blastomeres is provided by the translation of maternal *oep* mRNA. The mRNA is later degraded throughout the entire embryo, probably owing to the use of codons that reduce mRNA stability. This results in the loss of mesendodermal competence in the prospective ectoderm. Although the localized production and limited reach of Nodal signals, together with the action of Nodal inhibitors, restrict the range of Nodal signaling such that cells in the prospective ectoderm do not usually receive Nodal signal (Bell et al., 2003; Chen and Schier, 2002; Muller et al., 2012; van Boxtel et al., 2015; Wang et al., 2016), the loss of *oep* might confer robustness to the system. Indeed, although *oep* overexpression does not result in a dramatic developmental phenotype (Zhang et al.,

1998), extending the window of *oep* expression does extend the expression domain of the direct Nodal target *bhik* (Fig. S5).

The loss of mesendodermal competence caused by reduced expression of the Nodal co-receptor constitutes a different mechanism to those observed in previous studies, in which changes in cytoplasm and nucleus were shown to play a role in the loss of competence (Dupont et al., 2005; Grimm and Gurdon, 2002; Lim et al., 2013; Shiomi et al., 2017; Steinbach et al., 1997). Our observation that mesendodermal genes can still be activated when Oep is bypassed suggests that, at least in zebrafish, the cytoplasmic and nuclear components of the pathway are still intact when competence to respond to Nodal is lost. Interestingly, we did observe a decrease in the strength of ectopic *ntl* induction at 75% epiboly, which might suggest that, at this stage, changes in cytoplasmic and nuclear components of the pathway, or the chromatin structure of target genes, also affect the response to Nodal signaling.

Taken together, we show that reduced expression of the Nodal co-receptor *oep* in the prospective ectoderm results in the loss of mesendodermal competence. The loss of competence as a result of reduced levels of a receptor represents a simple, cell-autonomous mechanism. Because of the very upstream position of receptors in signaling pathways, such a mechanism ensures a global effect on the responsiveness to signals during development. Loss of a receptor has previously been shown to regulate the competence of embryonic cardiomyocytes to undergo Purkinje fiber differentiation during avian cardiogenesis (Kanzawa et al., 2002). Future studies will reveal how widely the loss of a receptor is used to modulate competence during development.

MATERIALS AND METHODS

Zebrafish
Wild-type (TLAB) *Danio rerio* embryos were maintained and raised under standard conditions, in accordance with the declaration of Helsinki and the ethical standards of European and German animal welfare legislation.

mRNA and protein injections
mRNAs encoding OptoAcvRI and II, Oep and EGFP were synthesized *in vitro*, purified, and injected into 1-cell stage embryos. Nodal and Activin A protein were obtained commercially and injected into the intercellular space at the indicated stages. For details, including analysis of the *oep* overexpression phenotype, see the supplementary Materials and Methods.

Optogenetic activation of Nodal signaling
Embryos were placed in a custom-made illumination chamber (Fig. S2) providing 470 nm LED light (10 µW mm^{-2}) in 20 s on/20 s off light pulses for 1.5 h, after which they were fixed. Control siblings were kept in a light-tight box next to the light-induced embryos.

In situ hybridization
Whole-mount mRNA *in situ* hybridization was performed as described (Thisse and Thisse, 2008). For details, see the supplementary Materials and Methods.

Transcription inhibition
Transcription was inhibited by soaking embryos in Danieu's medium containing 5 µg/ml flavopiridol (Enzo Life Sciences, ALX-430-161) in 0.1% DMSO. Control embryos were soaked in Danieu's medium containing 0.1% DMSO.

Quantitative RT-PCR (RT-qPCR)
Total RNA was extracted from 25 embryos, genomic DNA removed and cDNA synthesized from 1 µg total RNA. RT-PCRs were performed in technical duplicate. For details, see the supplementary Materials and Methods.

Author contributions
Conceptualization: P.V., N.L.V.; Methodology: P.V., S.P.; Formal analysis: P.V., N.L.V.; Investigation: P.V.; Resources: N.L.V.; Data curation: P.V.; Writing - original draft: P.V., N.L.V.; Writing - review & editing: P.V., N.L.V.; Visualization: P.V.; Supervision: N.L.V.; Funding acquisition: N.L.V.

Supplementary information
Supplementary information available online at
http://dev.biologists.org/lookup/doi/10.1242/dev.158832.supplemental

References
Bazzini, A. A., del Viso, F., Moreno-Mateos, M. A., Johnstone, T. G., Vejnar, C. E., Qin, Y., Yao, J., Khokha, M. K. and Giraldez, A. J. (2016). Codon identity regulates mRNA stability and translation efficiency during the maternal-to-zygotic transition. *EMBO J.* **35**, 2087-2103.

Bell, E., Munoz-Sanjuan, I., Altmann, C. R., Vonica, A. and Brivanlou, A. H. (2003). Cell fate specification and competence by Coco, a maternal BMP, TGFbeta and Wnt inhibitor. *Development* **130**, 1381-1389.

Bennett, J. T., Joubin, K., Cheng, S., Aanstad, P., Herwig, R., Clark, M., Lehrach, H. and Schier, A. F. (2007). Nodal signaling activates differentiation genes during zebrafish gastrulation. *Dev. Biol.* **304**, 525-540.

Bensaude, O. (2011). Inhibiting eukaryotic transcription: which compound to choose? How to evaluate its activity? *Transcription* **2**, 103-108.

Chen, Y. and Schier, A. F. (2002). Lefty proteins are long-range inhibitors of squint-mediated nodal signaling. *Curr. Biol.* **12**, 2124-2128.

Cheng, S. K., Olale, F., Bennett, J. T., Brivanlou, A. H. and Schier, A. F. (2003). EGF-CFC proteins are essential coreceptors for the TGF-beta signals Vg1 and GDF1. *Genes Dev.* **17**, 31-36.

Chu, J. and Shen, M. M. (2010). Functional redundancy of EGF-CFC genes in epiblast and extraembryonic patterning during early mouse embryogenesis. *Dev. Biol.* **342**, 63-73.

Dahle, O., Kumar, A. and Kuehn, M. R. (2010). Nodal signaling recruits the histone demethylase Jmjd3 to counteract polycomb-mediated repression at target genes. *Sci. Signal.* **3**, ra48.

Dorey, K. and Hill, C. S. (2006). A novel Cripto-related protein reveals an essential role for EGF-CFCs in Nodal signalling in Xenopus embryos. *Dev. Biol.* **292**, 303-316.

Dubrulle, J., Jordan, B. M., Akhmetova, L., Farrell, J. A., Kim, S.-H., Solnica-Krezel, L. and Schier, A. F. (2015). Response to Nodal morphogen gradient is determined by the kinetics of target gene induction. *eLife* **4**, e05042.

Dupont, S., Zacchigna, L., Cordenonsi, M., Soligo, S., Adorno, M., Rugge, M. and Piccolo, S. (2005). Germ-layer specification and control of cell growth by Ectodermin, a Smad4 ubiquitin ligase. *Cell* **121**, 87-99.

Feldman, B., Gates, M. A., Egan, E. S., Dougan, S. T., Rennebeck, G., Sirotkin, H. I., Schier, A. F. and Talbot, W. S. (1998). Zebrafish organizer development and germ-layer formation require nodal-related signals. *Nature* **395**, 181-185.

Feldman, B., Dougan, S. T., Schier, A. F. and Talbot, W. S. (2000). Nodal-related signals establish mesendodermal fate and trunk neural identity in zebrafish. *Curr. Biol.* **10**, 531-534.

Fleming, B. M., Yelin, R., James, R. G. and Schultheiss, T. M. (2013). A role for Vg1/Nodal signaling in specification of the intermediate mesoderm. *Development* **140**, 1819-1829.

Gilbert, S. F. (2010). *Developmental Biology*, 9th edn. Sunderland, MA: Sinauer Associates.

Giraldez, A. J., Mishima, Y., Rihel, J., Grocock, R. J., Van Dongen, S., Inoue, K., Enright, A. J. and Schier, A. F. (2006). Zebrafish MiR-430 promotes deadenylation and clearance of maternal mRNAs. *Science* **312**, 75-79.

Grainger, R. M. and Gurdon, J. B. (1989). Loss of competence in amphibian induction can take place in single nondividing cells. *Proc. Natl. Acad. Sci. USA* **86**, 1900-1904.

Grimm, O. H. and Gurdon, J. B. (2002). Nuclear exclusion of Smad2 is a mechanism leading to loss of competence. *Nat. Cell Biol.* **4**, 519-522.

Gritsman, K., Zhang, J., Cheng, S., Heckscher, E., Talbot, W. S. and Schier, A. F. (1999). The EGF-CFC protein one-eyed pinhead is essential for nodal signaling. *Cell* **97**, 121-132.

Ho, R. K. and Kimmel, C. B. (1993). Commitment of cell fate in the early zebrafish embryo. *Science* **261**, 109-111.

Kanzawa, N., Poma, C. P., Takebayashi-Suzuki, K., Diaz, K. G., Layliev, J. and Mikawa, T. (2002). Competency of embryonic cardiomyocytes to undergo Purkinje fiber differentiation is regulated by endothelin receptor expression. *Development* **129**, 3185-3194.

Kontur, C. and Giraldez, A. (2017). RNA methylation clears the way. *Dev. Cell* **40**, 427-428.

Kunwar, P. S., Zimmerman, S., Bennett, J. T., Chen, Y., Whitman, M. and Schier, A. F. (2003). Mixer/Bon and FoxH1/Sur have overlapping and divergent roles in Nodal signaling and mesendoderm induction. *Development* **130**, 5589-5599.

Lim, C. Y., Reversade, B., Knowles, B. B. and Solter, D. (2013). Optimal histone H3 to linker histone H1 chromatin ratio is vital for mesodermal competence in Xenopus. *Development* **140**, 853-860.

Morikawa, M., Koinuma, D., Miyazono, K. and Heldin, C.-H. (2013). Genome-wide mechanisms of Smad binding. *Oncogene* **32**, 1609-1615.

Muller, P., Rogers, K. W., Jordan, B. M., Lee, J. S., Robson, D., Ramanathan, S. and Schier, A. F. (2012). Differential diffusivity of Nodal and Lefty underlies a reaction-diffusion patterning system. *Science* **336**, 721-724.

Poulain, M. and Lepage, T. (2002). Mezzo, a paired-like homeobox protein is an immediate target of Nodal signalling and regulates endoderm specification in zebrafish. *Development* **129**, 4901-4914.

Sako, K., Pradhan, S. J., Barone, V., Inglés-Prieto, A., Müller, P., Ruprecht, V., Čapek, D., Galande, S., Janovjak, H. and Heisenberg, C.-P. (2016). Optogenetic control of nodal signaling reveals a temporal pattern of nodal signaling regulating cell fate specification during gastrulation. *Cell Rep.* **16**, 866-877.

Schier, A. F. (2009). Nodal morphogens. *Cold Spring Harb. Perspect. Biol.* **1**, a003459.

Schier, A. F., Neuhauss, S. C., Helde, K. A., Talbot, W. S. and Driever, W. (1997). The one-eyed pinhead gene functions in mesoderm and endoderm formation in zebrafish and interacts with no tail. *Development* **124**, 327-342.

Schulte-Merker, S., van Eeden, F. J., Halpern, M. E., Kimmel, C. B. and Nüsslein-Volhard, C. (1994). no tail (ntl) is the zebrafish homologue of the mouse T (Brachyury) gene. *Development* **120**, 1009-1015.

Shiomi, T., Muto, A., Hozumi, S., Kimura, H. and Kikuchi, Y. (2017). Histone H3 Lysine 27 trimethylation leads to loss of mesendodermal competence during gastrulation in zebrafish ectodermal cells. *Zoolog. Sci.* **34**, 64-71.

Slagle, C. E., Aoki, T. and Burdine, R. D. (2011). Nodal-dependent mesendoderm specification requires the combinatorial activities of FoxH1 and Eomesodermin. *PLoS Genet.* **7**, e1002072.

Steinbach, O. C., Wolffe, A. P. and Rupp, R. A. W. (1997). Somatic linker histones cause loss of mesodermal competence in Xenopus. *Nature* **389**, 395-399.

Thisse, C. and Thisse, B. (2008). High-resolution in situ hybridization to whole-mount zebrafish embryos. *Nat. Protoc.* **3**, 59-69.

Thisse, B., Wright, C. V. E. and Thisse, C. (2000). Activin- and Nodal-related factors control antero-posterior patterning of the zebrafish embryo. *Nature* **403**, 425-428.

van Boxtel, A. L., Chesebro, J. E., Heliot, C., Ramel, M.-C., Stone, R. K. and Hill, C. S. (2015). A temporal window for signal activation dictates the dimensions of a nodal signaling domain. *Dev. Cell* **35**, 175-185.

Vogel, A. M. and Gerster, T. (1999). Promoter activity of the zebrafish bhikhari retroelement requires an intact activin signaling pathway. *Mech. Dev.* **85**, 133-146.

Wang, Y., Wang, X., Wohland, T. and Sampath, K. (2016). Extracellular interactions and ligand degradation shape the nodal morphogen gradient. *eLife* **5**, e13879.

Xi, Q., Wang, Z., Zaromytidou, A.-I., Zhang, X. H.-F., Chow-Tsang, L.-F., Liu, J. X., Kim, H., Barlas, A., Manova-Todorova, K., Kaartinen, V. et al. (2011). A poised chromatin platform for TGF-beta access to master regulators. *Cell* **147**, 1511-1524.

Yang, Q., Liu, X., Zhou, T., Cook, J., Nguyen, K. and Bai, X. (2016). RNA polymerase II pausing modulates hematopoietic stem cell emergence in zebrafish. *Blood* **128**, 1701-1710.

Zhang, J., Talbot, W. S. and Schier, A. F. (1998). Positional cloning identifies zebrafish one-eyed pinhead as a permissive EGF-related ligand required during gastrulation. *Cell* **92**, 241-251.

Zhao, B. S., Wang, X., Beadell, A. V., Lu, Z., Shi, H., Kuuspalu, A., Ho, R. K. and He, C. (2017). m6A-dependent maternal mRNA clearance facilitates zebrafish maternal-to-zygotic transition. *Nature* **542**, 475-478.

DEVELOPMENT

SUPPLEMENTARY MATERIAL

SUPPLEMENTARY MATERIAL AND METHODS

mRNA and protein injections

mRNA was synthetized using the mMessage mMachine Kit (Thermo Fisher Scientific) and purified using the Qiagen RNeasy kit. For optogenetic manipulation, 15 pg of *in vitro* transcribed mRNA encoding OptoAcvRI and II (Sako et al., 2016) was injected into 1-cell stage embryos under dim red light illumination. Upon injection, embryos were moved to the dark and any subsequent manipulation (sorting, cleaning) was performed under dim red light. For *oep* (Zhang et al., 1998) and *egfp*, 50 pg of mRNA was injected into 1-cell stage embryos. For induction experiments, either 100 pg of carrier-free recombinant human Nodal (rhNodal, R&D Systems, 3218-ND-025/CF) or 20 pg of recombinant human Activin A (Biolegend, BLD 592002) was injected.

In situ hybridization

Whole-mount mRNA *in situ* hybridization was performed as described before (Thisse and Thisse, 2008). For imaging, embryos were cleared in 100% MeOH, rehydrated, mounted in 55% glycerol in PBT and documented using a stereomicroscope (Leica MC170 with Leica MC170 HD camera). For *ntl*, *sox2* and *sox3*, previously published probes were used (Bennett et al., 2007). For *sebox*, part of the coding sequence was amplified using the following primers: Fwd 5'-ATGCGGACGACTGCGCTT-3'; Rev 5'-TTAGCACTCTTCCAGATTAGTG-3'.

Quantitative RT-PCR

Twenty-five embryos were snap-frozen in liquid nitrogen. Total RNA was extracted using the RNeasy Mini Kit (Qiagen) and genomic DNA was removed using the DNA-free kit (Thermo Fisher Scientific AM1906). cDNA was synthetized from 1 µg total RNA with the iScript cDNA synthesis kit (Bio-Rad) and diluted 1/10 after which 5 µl was used for qPCR performed in technical duplicate on the LightCycler® 96 System (Roche). Primers used for qPCR were: *oep* 5th intron: Fwd 5'-

GTGGTGAGTTTACTGATGCAC-3'; Rev 5'-AATCCGATTCAATGATCTATGC-3'. *eif4g2a*: Fwd 5'-GAGATGTATGCCACTGATGAT-3'; Rev: 5'-GCGCAGTAACATTCCTTTAG-3'.

Analysis of Oep overexpression phenotype

Embryos injected with 50pg *oep* mRNA or 50 pg *egpf* mRNA were fixed at 60% epiboly and *bhik* expression was analyzed by whole-mount *in situ* hybridization. Only embryos of the exact same developmental stage (based on prechordal plate extension) were imaged using a stereomicroscope (Leica MC170 with Leica MC170 HD camera) in side view. To guarantee comparable illumination conditions during imaging, the *oep-* and *egfp-*mRNA injected embryos were documented in an alternating fashion on the same plate, in the same imaging session, and with the same camera settings. For signal quantification, a rectangular area of ~270 x160um on the lateral side of the embryo was used.

Analysis of codon usage

The stability score of a given transcript was calculated by averaging the codon stabilization coefficient over all codons in the coding sequence. The codon stabilization coefficient values were taken from Figure 1D in (Bazzini et al., 2016). The classification of stabilizing (green: AAG, GAC, GGA, GGC, GAU, GCC, GGU, GAG) and destabilizing (red: UCA, AGG, AUA, CAU, UGG, AGC, UCU, UUG, CAC, CAA, UUA, AGU, UGC, UGU) codons is based on Figure 2E in (Bazzini et al., 2016).
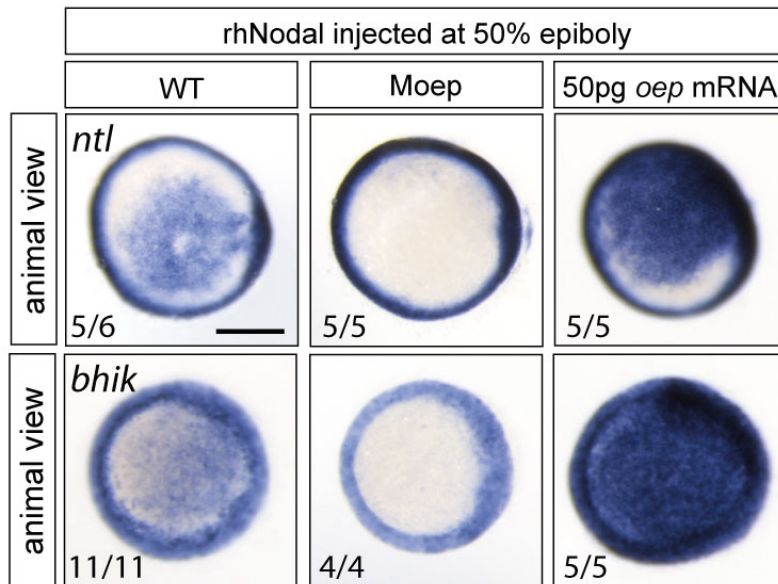
Figure S1. The effect of intercellular injection of rhNodal on target gene expression is mediated by Nodal signaling. Intercellular injection of rhNodal results in the ectopic expression of Nodal target genes *ntl* and *bhik* in wildtype embryos, but not in maternal *oep* (Moep) mutants. Elevated levels of *oep* result in higher levels of *ntl* and *bhik* expression upon intercellular injection of rhNodal. The number of embryos with the indicated expression pattern per total number of embryos examined in one biological replicate is shown. Scale bar 250 μm.
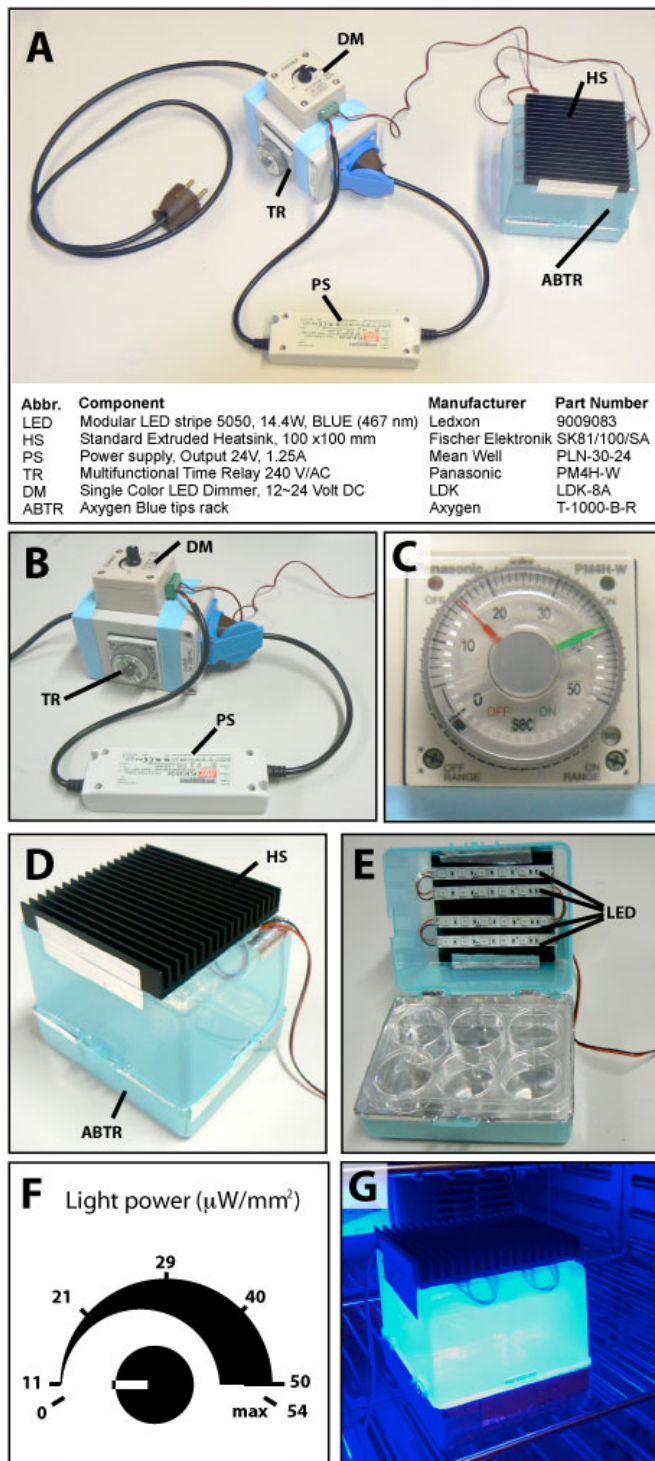
Figure S2. A simple, custom-made, optogenetic chamber. A) An overview of the device and specification of its construction parts. **B)** A close-up of the power supply components. A 230V AC passes through a Multifunctional Time Relay 240V/AC (TR) that allows setting the time intervals for ON/OFF light pulses (see panel C). Then the 240 V AC is transformed to 24V DC by power supply unit (PS) and is passed to a Single-Color LED Dimmer (DM), from which it continues to four stripes of 467 nm LED diodes. **C)** A detail of the time relay allowing easy setting of ON/OFF time intervals for the light pulse. 15s OFF and 40s ON pulse intervals are shown as an example; 20/20s ON/OFF were used in the experiments in this study. **D)** The chamber is constructed from a blue-tip rack in which the bottom was substituted by a 100x100mm heatsink to avoid overheating of the sample by the heat produced by the diodes. **E)** A detail of the inside of the chamber holding a six-well plate as typically used in the experiments. The LED stripes are glued directly to the heatsink. The chamber is coated by aluminum foil to maximize the amount of light reaching the sample. **F)** The dimmer knob is used to set the light power at the bottom of a 6-well plate. Values given are estimates based on our experience. **G)** The optogenetic chamber during operation inside of a 28.5 °C incubator with blue light ON.
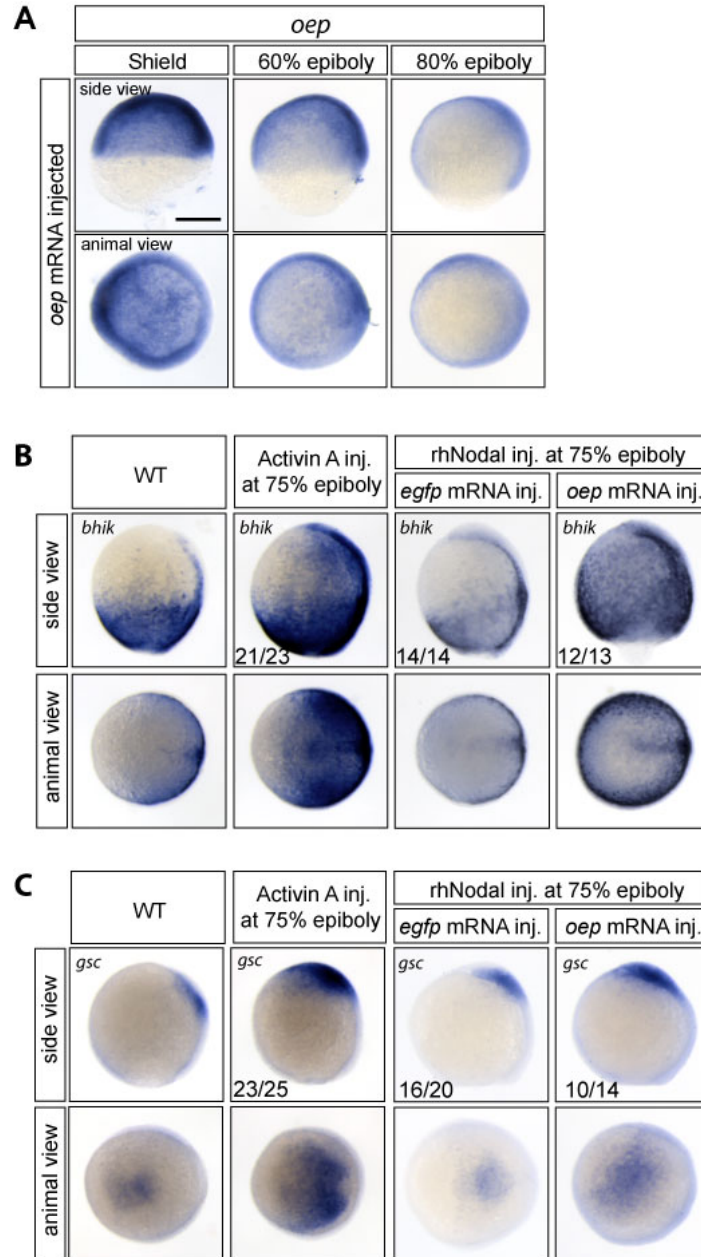
Figure S3. Oep overexpression prolongs the window of induction of Nodal target genes *bhik* and *gsc* in prospective ectoderm.

A) Injection of 50pg *oep* mRNA at the 1-cell stage extends the expression level of *oep* to late gastrulation stages (compare to Fig. 3A). **(B,C)** Both *bhik* **(B)** and *gsc* **(C)** show the same induction response as *ntl*. At 75% epiboly, both genes can be ectopically induced by Activin A injection but not by rhNodal injection into *egfp* mRNA-injected embryos. When *oep* is overexpressed, rhNodal injection also results in ectopic expression of target genes. The number of embryos with the indicated expression pattern per total number of embryos examined in one biological replicate is shown. Scale bar 250 μm.

A
TTGTCATGTTCGCCCCTTTTATTTTACACCGCCTGCTGTAAatgagttttcctaatggga
tagttcacccaaacaaagaaatgatctcccctgttgaacgcagaagaagatactttgaa
aaatgctg**gcactt**gacttccatagtaggggaaacattactatggaagtgaaccagcatt
tctcttttgtgcccaagagaaggaagcagctctcaaataggtttttaaaccgttgaaggat
gagtaaatgtgttcattttcgtgtgaactatccctttaacaaacagaaagcggtttttatt
ttagattttttttctgtctgacaggttcgggcagcatttattggtggcactgaaatgtgtt
tttgcttccagtggaagtctaactagctgtgttaagagctgtttagtgaaggaacatgta
tataggatttatattgaaaatatattgtgtgtgtgtgtcagtgcgccgccgagccaaatg
aattctgtccttttctatgtctctgcgtgaatttattgtaccagagagagtgcgccggct
gaaagcaaagcattttcatcgtctgtatctgcaaatacacgtgtttttattttaatacatg
tcatcttaacagtgagctgtggcttttgtttttaagttctcgctagtcgaatgtccttat
ttgtgctccacaactttcatttgccgtgcttgttaatggagaaggagtcagataatgcag
agatagcctgtgatttgttgacctttcggctattttctcttatcttatacaaacaagtcg
tccatttggccaatcaatctgggtggctggagcgaccgtcttgaccttcttgatgtactg
taacgctccgtatgattgagcgaattaatttgtctcatccaattaaaactcgcatcaaaa
acccagatgactgactgtttactgacttcaattaggcagtttatcatggatgctgaaaat
tagattggagctcaggcgataataagccgtgacatccaaacaagacctttatggagattc
aggagtaaaacactactttgccaagtttttggaaacaataattagaatgtctgtttggaga
ttataacatttgatgacattaattcaagctcatgtttac

B

C
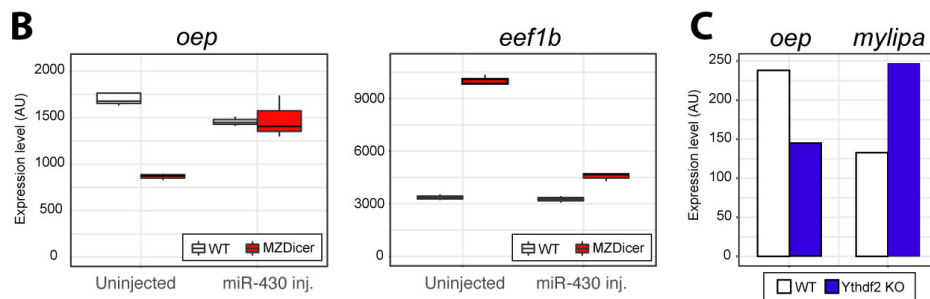
Figure S4. Maternal oep mRNA degradation does not depend on miR-430 and m⁶A-dependent mRNA decay

A) In the 3'UTR of the *oep* transcript, only a single seed sequence for miR-430 is present. Magenta capital letters indicate the 3' end of the coding sequence. Lowercase black letters indicate the 3'UTR, as retrieved from Ensembl zebrafish genome database (ENSDARG00000035095.1). Black italic lower case letters indicate the maximal span of 3'UTR, as identified in (Pauli et al., 2012). The single miR-430 target sequence is indicated in blue. **B)** Expression levels of *oep* and *eef1b* transcripts in wild-type and MZdicer mutant embryos, with and without rescue by miR-430 injection. Expression data taken from Gene Expression Omnibus accession number GSE4201 related to (Giraldez et al., 2006). *eef1b* (a gene that is regulated by miR-430) shows increased expression in MZdicer mutants, an effect that is lost upon injection of miR-430. In contrast, *oep* expression is reduced in MZdicer mutants. **C)** Expression levels of *oep* and *mylipa* in wild-type and *ythdf2* mutant embryos at 4hpf. Expression values taken from the dataset published in (Zhao et al., 2017). While *mylipa* shows increased expression in *ythdf2* mutant due to the impairment of m⁶A-dependent mRNA decay (Zhao et al., 2017), *oep* expression is decreased.
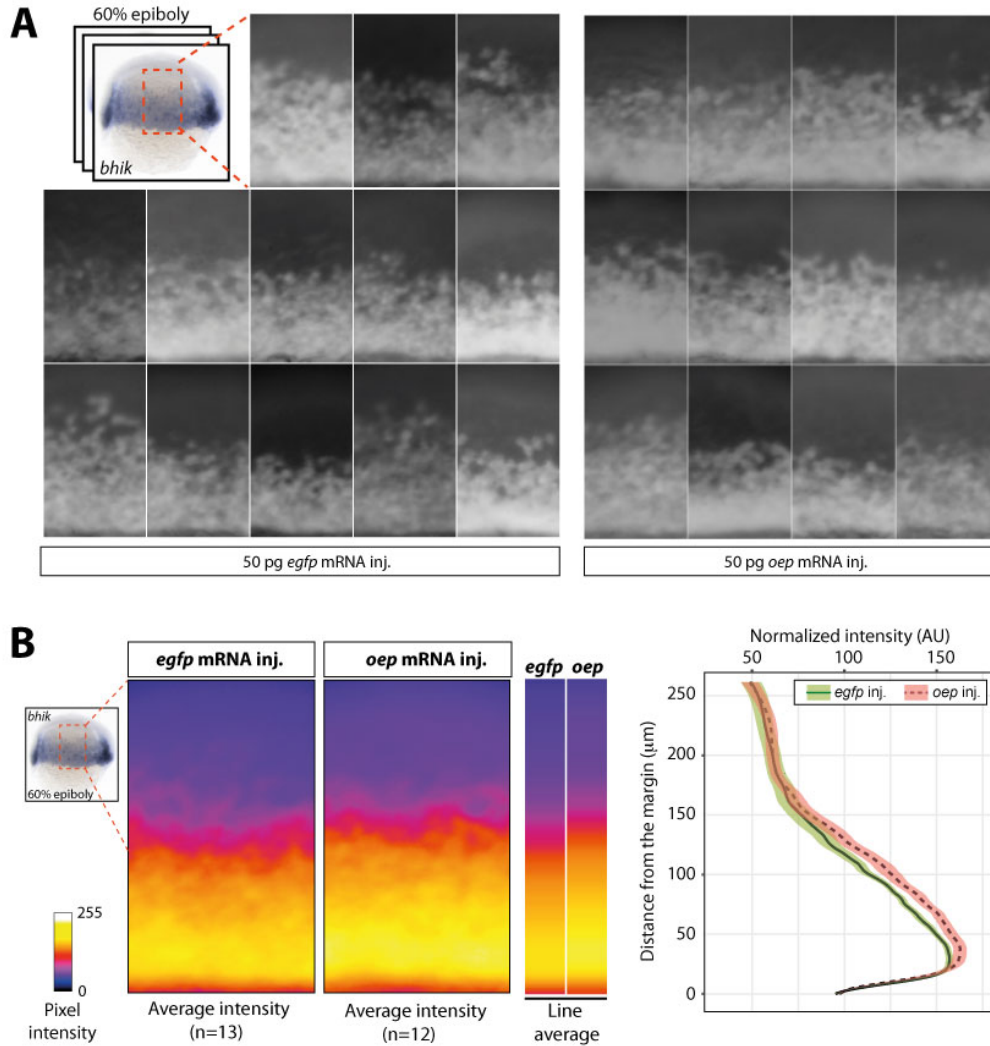
Figure S5. Overexpression of *oep* results in expansion of *bhik* expression domain towards the animal pole.

A) Lateral view of the expression of *bhik* in individual 60% epiboly embryos injected with *egfp* or *oep* mRNA. **B)** Signal intensity of the lateral area averaged over multiple embryos is shown in the heatmap panels. Average intensity of *bhik* staining profiles along the animal-vegetal axis for both treatments are shown in heatmap bars. Corresponding values are plotted in the graph. Colored envelopes of the curves represent the standard error of the mean, based on 12 (*oep*) and 13 (*egfp*) embryos. *bhik* expression is similar in *oep*- and *egfp*-injected most animally and vegetally, but in *oep*-injected embryos, the average intensity is higher in the mesendoderm area, and the expression domain is extended towards the animal pole. Shown is a representative example of three biological replicates. Although this expansion of the reach of Nodal signaling does not impede development ((Zhang et al., 1998), this study), the decrease in *oep* expression might be relevant under altered environmental conditions.

SUPPLEMENTARY REFERENCES

Bazzini, A. A., Del Viso, F., Moreno-Mateos, M. A., Johnstone, T. G., Vejnar, C. E., Qin, Y., Yao, J., Khokha, M. K. and Giraldez, A. J. (2016). Codon identity regulates mRNA stability and translation efficiency during the maternal-to-zygotic transition. *EMBO J* **35**, 2087-2103.

Bennett, J. T., Joubin, K., Cheng, S., Aanstad, P., Herwig, R., Clark, M., Lehrach, H. and Schier, A. F. (2007). Nodal signaling activates differentiation genes during zebrafish gastrulation. *Developmental Biology* **304**, 525-540.

Giraldez, A. J., Mishima, Y., Rihel, J., Grocock, R. J., Van Dongen, S., Inoue, K., Enright, A. J. and Schier, A. F. (2006). Zebrafish MiR-430 promotes deadenylation and clearance of maternal mRNAs. *Science* **312**, 75-79.

Pauli, A., Valen, E., Lin, M. F., Garber, M., Vastenhouw, N. L., Levin, J. Z., Fan, L., Sandelin, A., Rinn, J. L., Regev, A., et al. (2012). Systematic identification of long noncoding RNAs expressed during zebrafish embryogenesis. *Genome research* **22**, 577-591.

Sako, K., Pradhan, S. J., Barone, V., Ingles-Prieto, A., Muller, P., Ruprecht, V., Capek, D., Galande, S., Janovjak, H. and Heisenberg, C. P. (2016). Optogenetic Control of Nodal Signaling Reveals a Temporal Pattern of Nodal Signaling Regulating Cell Fate Specification during Gastrulation. *Cell Rep* **16**, 866-877.

Thisse, C. and Thisse, B. (2008). High-resolution in situ hybridization to whole-mount zebrafish embryos. *Nature protocols* **3**, 59-69.

Zhang, J., Talbot, W. S. and Schier, A. F. (1998). Positional cloning identifies zebrafish one-eyed pinhead as a permissive EGF-related ligand required during gastrulation. *Cell* **92**, 241-251.

Zhao, B. S., Wang, X., Beadell, A. V., Lu, Z., Shi, H., Kuuspalu, A., Ho, R. K. and He, C. (2017). m6A-dependent maternal mRNA clearance facilitates zebrafish maternal-to-zygotic transition. *Nature* **542**, 475-478.